

NACA RM E56D23a



RESEARCH MEMORANDUM

A VARIABLE-GEOMETRY ANNULAR CASCADE-TYPE INLET AT
MACH NUMBERS OF 1.9 AND 3.05

By James F. Connors and Rudolph C. Meyer

Lewis Flight Propulsion Laboratory

Cleveland, Ohio

CLASSIFICATION CHANGED

UNCLASSIFIED

To _____

By authority of *Assoc TPA & H. H. H. H. H.* Date *7-22-57*

01B 12-4-57

CLASSIFIED DOCUMENT

This material contains information affecting the National Defense of the United States within the meaning of the espionage laws, Title 18, U.S.C., Sections 793 and 794, the transmission or revelation of which in any manner to an unauthorized person is prohibited by law.

NATIONAL ADVISORY COMMITTEE FOR AERONAUTICS

WASHINGTON

July 24, 1956

UNCLASSIFIED



NATIONAL ADVISORY COMMITTEE FOR AERONAUTICS

RESEARCH MEMORANDUM

A VARIABLE-GEOMETRY ANNULAR CASCADE-TYPE INLET AT

MACH NUMBERS OF 1.9 AND 3.05

By James F. Connors and Rudolph C. Meyer

SUMMARY

An axisymmetric variable-geometry cascade inlet has been proposed and demonstrated. By means of a translating spike, an annular double-passage cascade arrangement was formed at a Mach number of 1.9 and a single-passage configuration with an internal area discontinuity (vortex trap) was effected at a Mach number of 3.05.

This annular cascade inlet yielded total-pressure recoveries of 0.84 and 0.53 at Mach numbers of 1.9 and 3.05, respectively. Mass-flow ratios of approximately unity were obtained at both Mach numbers with only marginal subcritical stability ranges of mass-flow ratio (~ 0.03). Angles of attack up to 6° produced only moderate decreases in performance.

INTRODUCTION

For most applications to supersonic aircraft, inlets must operate efficiently over a range of Mach number. Up to the present time, most investigations on axisymmetric inlets at Mach numbers greater than 2.0 have been concerned primarily with fixed-geometry design-point studies. Consequently, little information is currently available on axisymmetric design techniques for variable Mach number operation.

For Mach numbers less than 2.0, simple spike translation appears to provide an adequate solution to the problem of axisymmetric variable-geometry design technique. For Mach numbers greater than 2.0, however, merely translating the spike necessitates the use of relatively high-drag cowls in order to avoid net internal-area contractions. In reference 1, a telescoping-spike technique was successful in producing a variable spike contour that would adjust with the Mach number. This arrangement, however, appears to involve a rather complex mechanism.

UNCLASSIFIED

The present investigation demonstrates a somewhat simpler axisymmetric variable-geometry technique. This design employs an annular cascade-type inlet with a translating spike, which is evaluated in detail at Mach numbers of 1.9 and 3.05. The inlet was designed to capture the maximum free-stream tube of air and to maintain attached shocks on the cowl at each Mach number. Basically, this inlet is shorter than the more conventional configurations because of a double-passage cascade arrangement at a Mach number of 1.9 and an internal area discontinuity (vortex trap) at a Mach number of 3.05.

Performance is evaluated in terms of pressure-recovery and mass-flow characteristics for angles of attack from 0° to 6° .

SYMBOLS

The following symbols are used in this report:

- M Mach number
m mass flow, slugs/sec
P total pressure, lb/sq ft
R duct radius at diffuser exit, ft
r local tube radius, ft.
 α angle of attack, deg

Subscripts:

- 1 local pitot
0 free stream
3 diffuser exit

APPARATUS AND PROCEDURE

The experiments were conducted in the Lewis 18- by 18-inch supersonic wind tunnels 1 and 2. In both facilities the stagnation temperature of the air was maintained at $150^\circ \pm 5^\circ$ F and the dew-point temperature at $-20^\circ \pm 5^\circ$ F. Tunnel 1 was operated at a Mach number of 1.9, a simulated pressure altitude of 45,000 feet, and a Reynolds number of 3.3×10^6 per foot. Tunnel 2 was operated at a Mach number of 3.05, a simulated pressure altitude of 82,000 feet, and a Reynolds number of 1.7×10^6 per foot.

A schematic drawing of the tunnel installation is presented in figure 1(a). The model was strut mounted off the tunnel wall. At the rear of the model a movable exit plug was used to vary the inlet back pressure. Provisions were incorporated in the strut to permit angle-of-attack variations up to 6° . A twin-mirror schlieren system was used to observe the inlet-air-flow patterns.

Design details of the variable-geometry annular cascade inlet are given in table I and are illustrated in figure 1(b) and in the photograph of figure 2. The inlet consists of a translating center spike with two concentric cowls. At a Mach number of 3.05 the spike is located in its most forward position and contacts the inner cowl to form a single, smooth continuous surface. The contoured isentropic spike is designed for this Mach number and focuses the resulting compression characteristics at the outer cowl lip. The flow is to be compressed nearly isentropically to a Mach number of 2.05 at the diffuser entrance. Internally, an area discontinuity occurs in the subsonic diffuser at the trailing edge of the inner cowl.

At the lower Mach numbers (e.g., at Mach number 1.9, fig. 1(b)), the spike is translated rearward, thus forming two concentric passages. The flow in the outer annulus is to be compressed through two oblique shocks (the second being generated by the inner cowl) and a normal shock at the diffuser entrance. The break point between the spike and the inner cowl was determined by the requirement that the second oblique shock intercept the lip of the outer cowl. The flow in the inner annulus is to be compressed through the conical shock off the spike with some isentropic turning and enough internal contraction to effect a pressure balance between the two flows at the point of confluence. This pressure equalization is desirable in order to minimize any twin-duct interaction.

In figure 1(c) the internal-area distribution is presented as a function of axial distance from the cowl lip. As described previously, an abrupt area discontinuity occurs at the trailing edge of the inner cowl with the Mach 3.05 configuration. Ideally, this step would serve as a vortex trap in order to reattach the flow to the centerbody at some station farther downstream. The associated subsonic mixing losses at the design critical condition are estimated to be approximately 2 percent of the local total pressure. Downstream of the common point, the area variation corresponds approximately to an equivalent 5° -conical area expansion.

Instrumentation consisted mainly of a 21-tube total-pressure rake and four wall static-pressure orifices located approximately $5\frac{1}{3}$ diameters downstream of the diffuser-exit station. An additional 13-tube rake

across one diameter of the duct was installed about 3/4-inch downstream of the end of the centerbody. This 13-tube rake was used only in the Mach 3.05 experiments to evaluate the total-pressure profiles after the flow had negotiated the upstream area discontinuity.

Total-pressure recovery was based on an area integration of the pressures measured by the 21-tube rake. With the assumption of unidimensional isentropic flow, mass flow was computed by means of the measured static pressure, the area at the rake station, and the known sonic discharge area at the plug.

RESULTS AND DISCUSSION

Diffuser performance characteristics of the variable-geometry annular cascade inlet are presented in figure 3. At Mach number 1.9 and zero angle of attack, a critical total-pressure recovery of 0.84 was obtained. This is comparable to a theoretical value of 0.90 based solely on shock losses. Critical mass flow was approximately unity and the subcritical stability range of mass-flow ratio $\Delta m/m_0$ was equal to 0.03. At Mach number 3.05 and zero angle of attack, a total-pressure recovery of 0.53 was obtained. This compares with a theoretical value of 0.68 based on shock losses and an estimated mixing loss due to the internal step. Critical mass flow was again approximately unity and the subcritical stability range $\Delta m/m_0$ was equal to 0.03.

The effect of angle of attack on performance is shown in figure 3 and summarized in the cross plot of figure 4. For both Mach numbers investigated, pressure-recovery, mass-flow, and subcritical stability range decreased only moderately with angles of attack up to 6°. A comparison with the performance of the axisymmetric telescoping-spike inlet of reference 1 is also included in figure 4. Recoveries were somewhat higher with the telescoping configuration at zero angle of attack. However, the variable-geometry annular cascade inlet is considerably more simple mechanically. The telescoping inlet also exhibited greater sensitivity to angle-of-attack effects at Mach number 3.05, which was indicated by the more rapid decrease in recovery with angle of attack. Although not shown in figure 4, a much greater subcritical stability range was realized with the telescoping-spike inlet.

At Mach number 3.05, total-pressure profiles across the diffuser exit during critical inlet operation are presented in figure 5. At this Mach number where an abrupt area discontinuity is in effect in the subsonic diffuser, the exit profiles appeared quite uniform with no

indication of separation at either zero or the 6° angle of attack. Theoretically, the mixing losses associated with the step were estimated at approximately 2 percent of the total pressure for the design critical condition. This rake (0.74 in. from the end of the diffuser centerbody) was not installed for the Mach 1.9 tests. At this lower speed the profile distortion problem should be less severe than at Mach 3.05 when both passages would be flowing full.

4085 Some schlieren photographs showing representative inlet-air-flow patterns are presented in figure 6. At Mach number 1.90 (fig. 6(a)), the zero-angle-of-attack supercritical shock patterns conform very closely to the design shock configuration (i.e., attached shocks occur on both the inner and outer cowl and appear to coalesce near the cowl lip). At critical and subcritical conditions, boundary-layer thickening and separation were observed on the spike. This boundary-layer effect increases with angle of attack. In this case, boundary-layer control, such as local suction in the vicinity of the throat, might lead to further improvements in performance. This possibility was not explored in the present series of tests. At Mach number 3.05 (fig. 6(b)), the patterns are quite conventional as would be expected since the external compression surface is the usual isentropic spike geometry. At zero angle of attack the compression waves coalesce at the lip with attached shocks on the cowl.

SUMMARY OF RESULTS

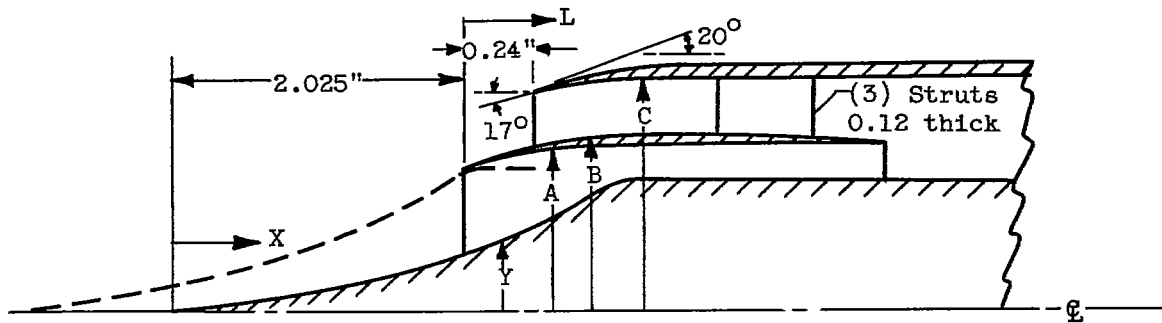
A variable-geometry annular cascade inlet was designed to form, by means of a translating center spike, a two-concentric-passage configuration at Mach number 1.9 and a single-passage arrangement with an internal area discontinuity (vortex trap) at Mach number 3.05. This inlet gave total-pressure recoveries of 0.84 and 0.53 at the Mach numbers 1.90 and 3.05, respectively. Unity mass-flow ratios were obtained at each Mach number with only marginal subcritical stability ranges of mass-flow ratio (~ 0.03). Angles of attack up to 6° produced only moderate decreases in performance.

Lewis Flight Propulsion Laboratory
National Advisory Committee for Aeronautics
Cleveland, Ohio, April 24, 1956

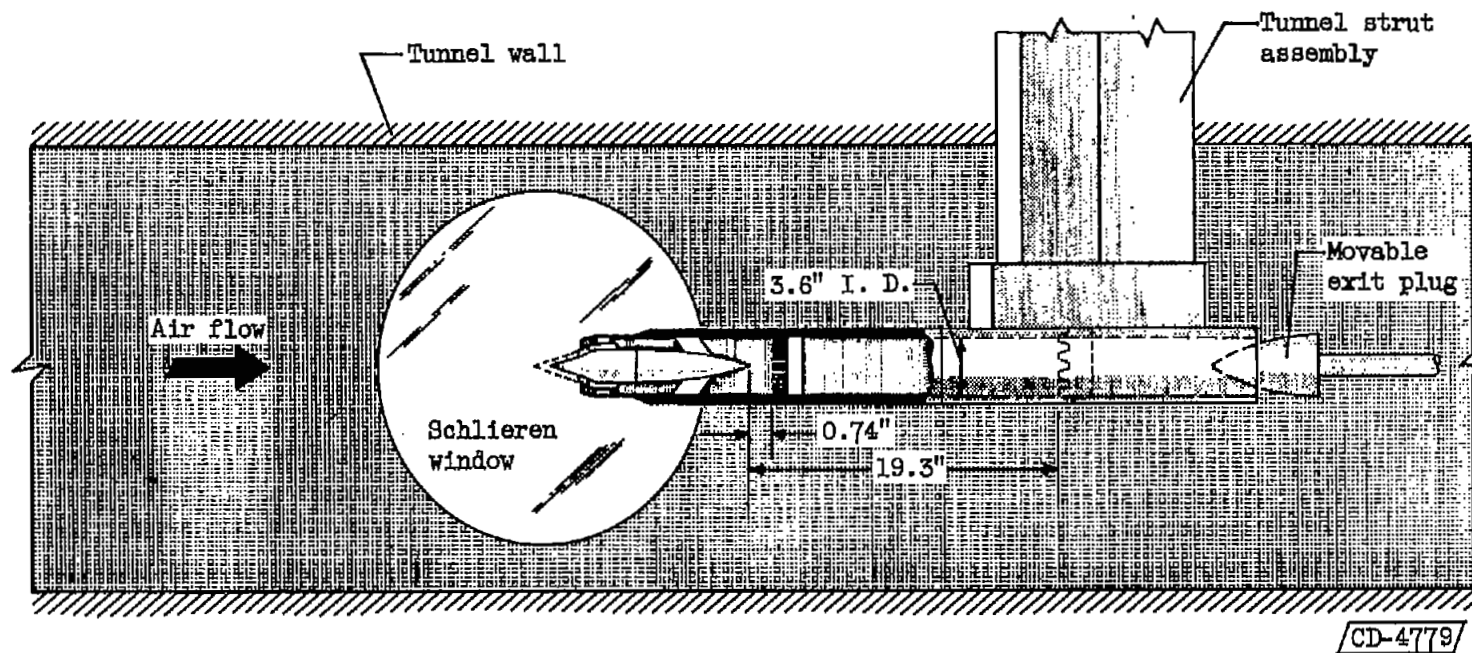
REFERENCE

1. Connors, James F., and Meyer, Rudolph C.: A Variable-Geometry Axisymmetric Supersonic Inlet with Telescoping Centerbody. NACA RM E55F30, 1955.

TABLE I. - DIMENSIONS OF VARIABLE-GEOMETRY INLET

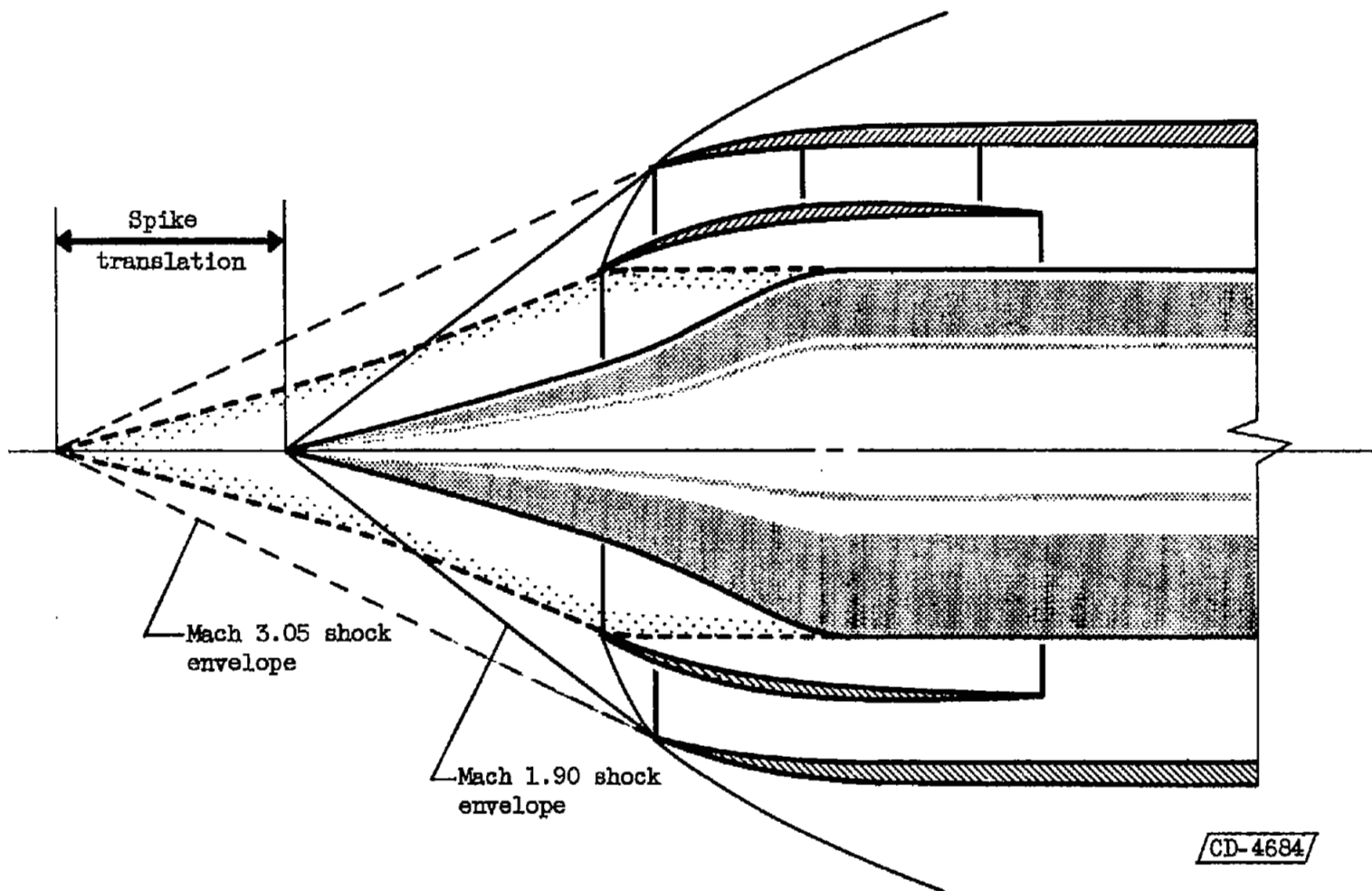


| Spike | | Island | | | Outer cowl | |
|-------|-------|--------|-------|-------|------------|-------|
| X | Y | L | A | B | L | C |
| 0.00 | 0.000 | 0.002 | 1.035 | 1.039 | 0.242 | 1.620 |
| 1.75 | .466 | .100 | 1.080 | ----- | .340 | 1.650 |
| 2.00 | .540 | .200 | 1.117 | ----- | .440 | 1.680 |
| 2.20 | .602 | .300 | 1.150 | ----- | .540 | 1.701 |
| 2.40 | .673 | .375 | ----- | 1.219 | .640 | 1.734 |
| 2.60 | .761 | .400 | 1.180 | ----- | .740 | 1.750 |
| 2.80 | .852 | .500 | 1.208 | 1.272 | .840 | 1.765 |
| 3.00 | .943 | .600 | 1.234 | 1.315 | .940 | 1.775 |
| 3.20 | 1.032 | .700 | 1.258 | 1.348 | 1.040 | 1.781 |
| 3.25 | 1.048 | .800 | 1.281 | 1.370 | 1.140 | 1.785 |
| 3.30 | 1.058 | .900 | 1.305 | 1.387 | 1.240 | 1.789 |
| 3.35 | 1.060 | 1.000 | 1.320 | 1.397 | 1.340 | 1.790 |
| 5.45 | 1.060 | 1.100 | 1.342 | 1.405 | 3.970 | 1.790 |
| | | 1.200 | 1.365 | 1.411 | 4.800 | 1.800 |
| | | 1.300 | 1.379 | 1.414 | | |
| | | 1.500 | ----- | 1.413 | | |
| | | 1.600 | ----- | 1.412 | | |
| | | 1.700 | ----- | 1.411 | | |
| | | 1.800 | ----- | 1.410 | | |
| | | 1.900 | ----- | 1.409 | | |
| | | 2.000 | ----- | 1.405 | | |
| | | 2.100 | ----- | 1.403 | | |
| | | 2.200 | ----- | 1.400 | | |
| | | 2.300 | ----- | 1.395 | | |
| | | 2.400 | ----- | 1.392 | | |
| | | 2.500 | ----- | 1.389 | | |
| | | 2.600 | ----- | 1.384 | | |
| | | 2.700 | ----- | 1.380 | | |
| | | 2.745 | 1.379 | 1.379 | | |



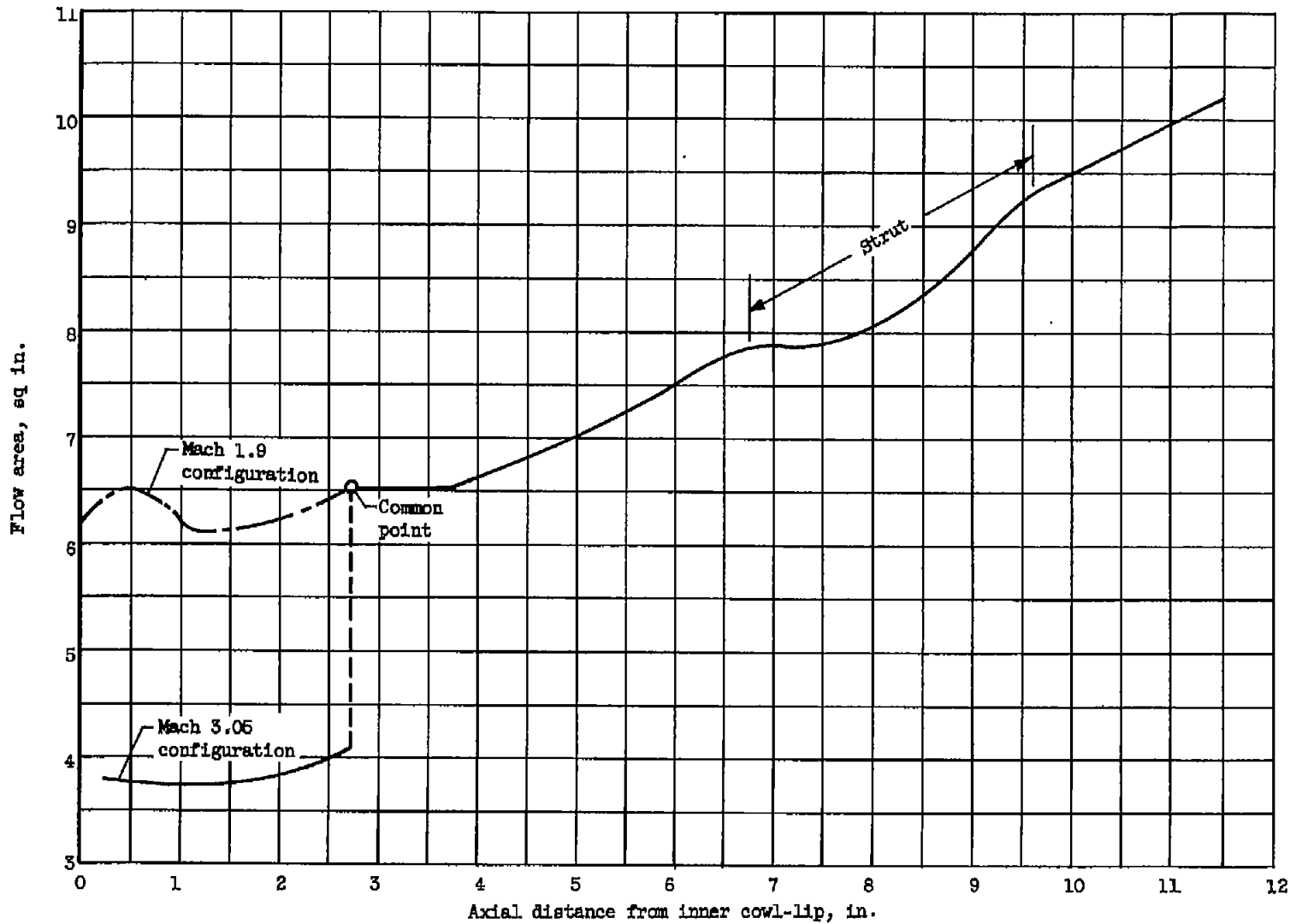
(a) Tunnel installation.

Figure 1. - Experimental apparatus for study of variable-geometry inlet.



(b) Schematic drawing of variable-geometry annular cascade-type inlet.

Figure 1. - Continued. Experimental apparatus for study of variable-geometry inlet.



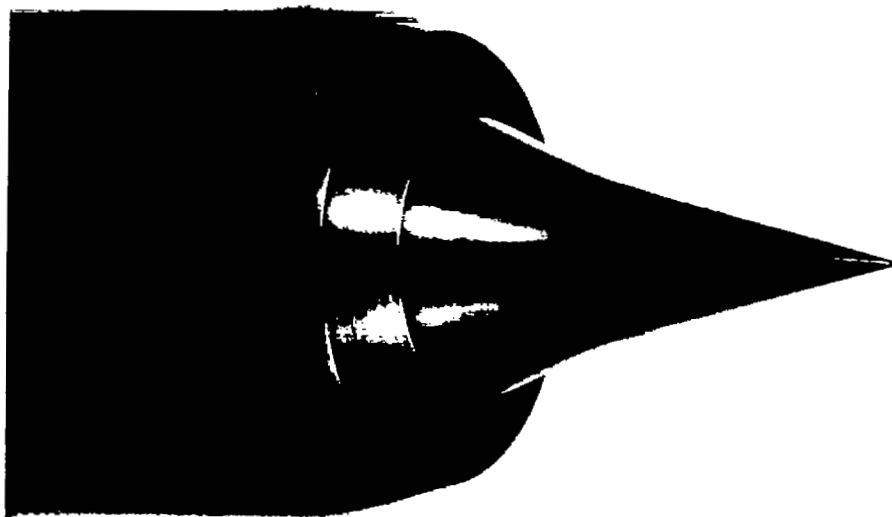
(c) Internal-area variation.

Figure 1. - Concluded. Experimental apparatus for study of variable-geometry inlet.



C-39690

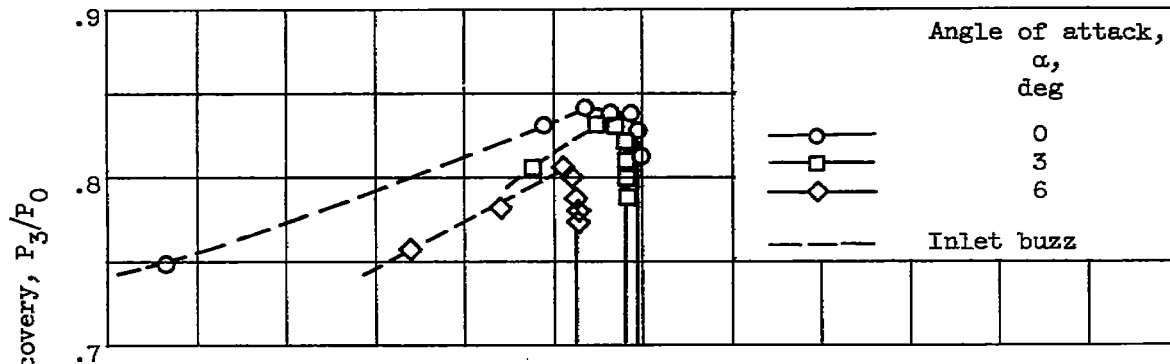
(a) Mach 1.90 configuration.



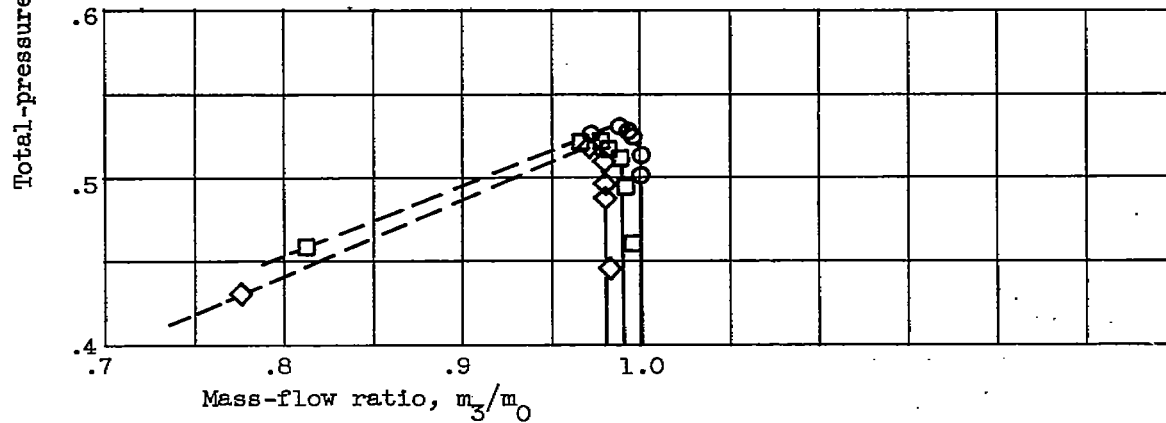
C-39691

(b) Mach 3.05 configuration.

Figure 2. - Variable-geometry annular cascade-type inlet.

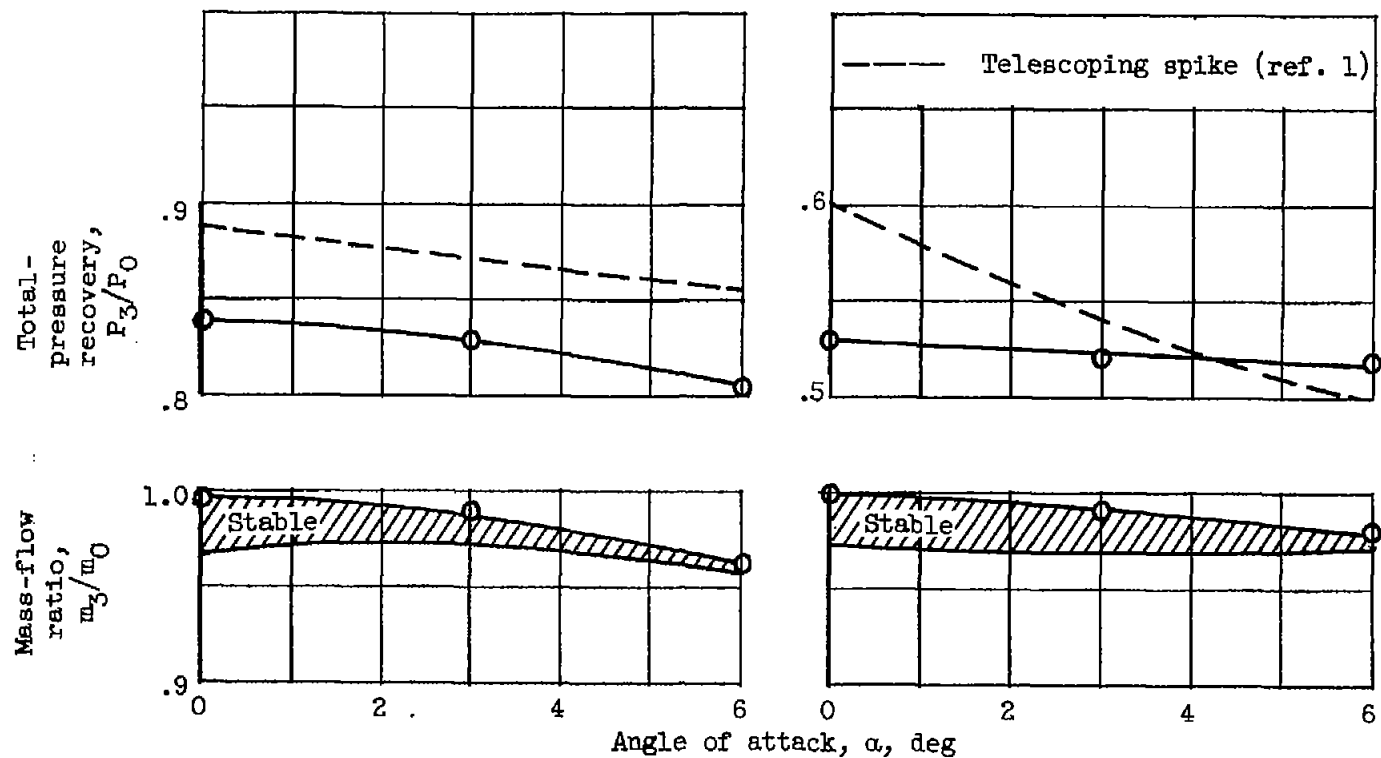


(a) Free-stream Mach number, 1.90.



(b) Free-stream Mach number, 3.05.

Figure 3. - Diffuser performance characteristics of variable-geometry annular cascade inlet.



(a) Free-stream Mach number, 1.90.

(b) Free-stream Mach number, 3.05.

Figure 4. - Effect of angle of attack on performance of variable-geometry annular cascade inlet.

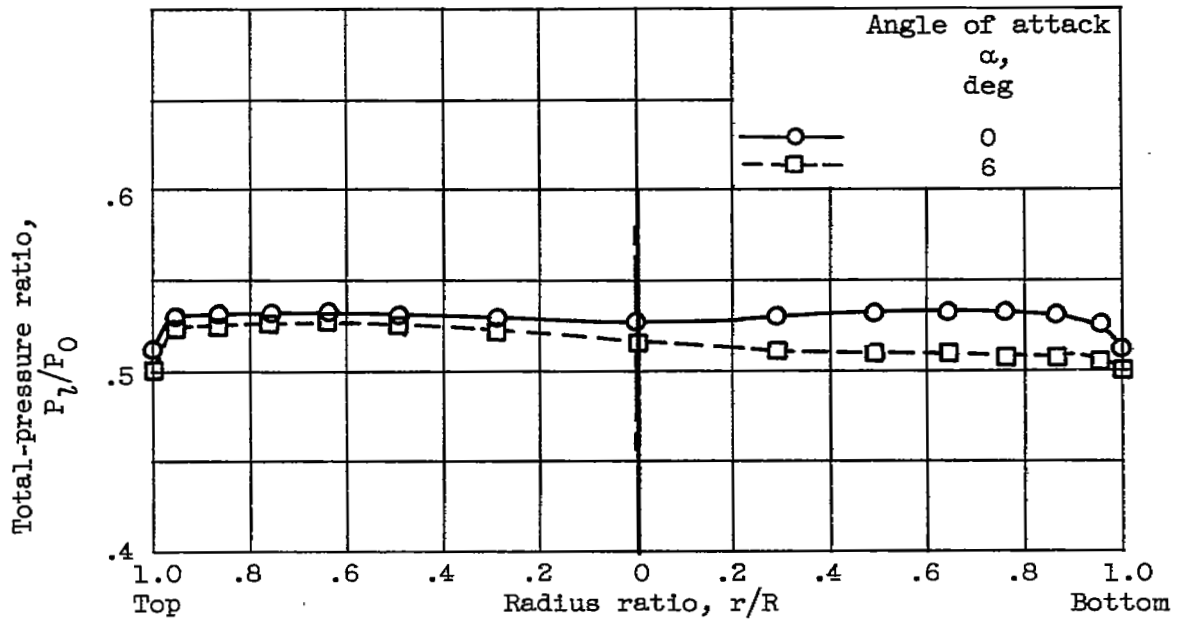
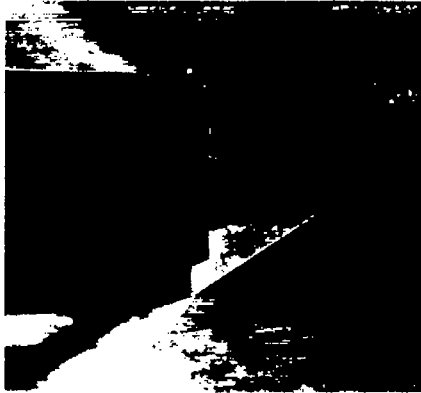


Figure 5. - Total-pressure distribution at diffuser exit (0.74-in. downstream of centerbody) during critical operation. Mach number, 3.05.



Supercritical mass flow



Minimum stable mass flow

Angle of attack, 0° .

Supercritical mass flow



Minimum stable mass flow

Angle of attack, 3° .

Supercritical mass flow



Minimum stable mass flow

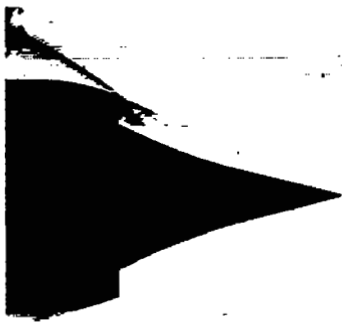
Angle of attack, 6° .

C-41840

(a) Free-stream Mach number, 1.90.

Figure 6. - Inlet flow patterns.

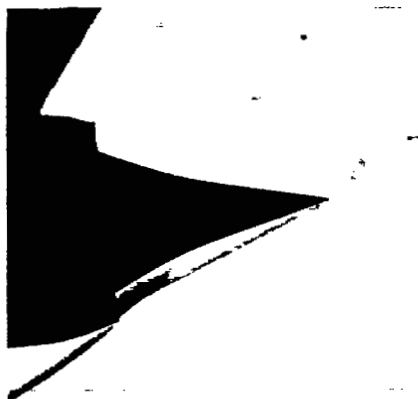
4085



Angle of attack, 0° .



Angle of attack, 3° .



C-41841

Angle of attack, 6° .

(b) Free-stream Mach number, 3.05.

Figure 6. - Concluded. Inlet flow patterns.

~~CONFIDENTIAL~~

NASA Technical Library



3 1176 01435 8486



~~CONFIDENTIAL~~